A Novel Vertical Directional Coupler Switch With Switching-Operation-Induced Section and Extinction-Ratio-Enhanced Section

Sung-Chan Cho, Byung-Min Jung, Boo-Gyoun Kim, *Member, IEEE*, Hyun Ha Hong, and Ali Shakouri, *Member, IEEE*

***Abstract*—A novel vertical directional coupler switch with a switching-operation-induced section and an extinction-ratio-enhanced section is proposed. Switching operation is achieved by changing the refractive indexes of both cores in the switching-operation-induced section, and an improvement of extinction ratios larger than 30 dB for both cross and bar states is achieved by controlling the asymmetry of the refractive indexes of two cores in the extinction-ratio-enhanced section without changing the refractive index of the inner-cladding layer between the two waveguides. The required refractive indexes for the cores in the switching-operation-induced and extinction-ratio-enhanced sections are calculated for various thickness of the inner-cladding layer.**

***Index Terms*—Extinction ratio, extinction-ratio-enhanced section, switching-operation-induced section, vertical directional coupler switch (VDCS), wafer fusion.**

I. Introduction

HIGH-SPEED optical-switching components for wide-bandwidth optical data stream play an important role in all-optical networks. The optical switch used in packet-switch applications should operate at high speeds ranging from microseconds to nanoseconds [1]. These high-speed switching operations can be achieved by the change of refractive index utilizing the electrooptic effect and the carrier injection (or depletion) [2], [3]. Major requirements for optical packet-switching elements are high extinction ratios, low polarization dependence, low loss, and scalability. Recently, a fused vertical coupler (FVC) with a very short coupling length of 62 μm was demonstrated [4]. Since the technique of wafer fusion can be used to combine waveguides fabricated on two different substrates into three-dimensional (3-D) structures, the problem of the separation of two vertical waveguides can be solved. The integration of $N \times N$ switching systems using, for example, the Basaline scheme to minimize the number of switching elements and stages is difficult to realize due to the loss at waveguide crossings between various stages [5]. However, in a FVC, this problem can be easily solved by separating the two waveguides with an air gap in the region where no coupling is required [see Fig. 1(a)]. In addition, the application of a bias at the fused layers will allow a change of mode overlap integral for switching purposes [4].

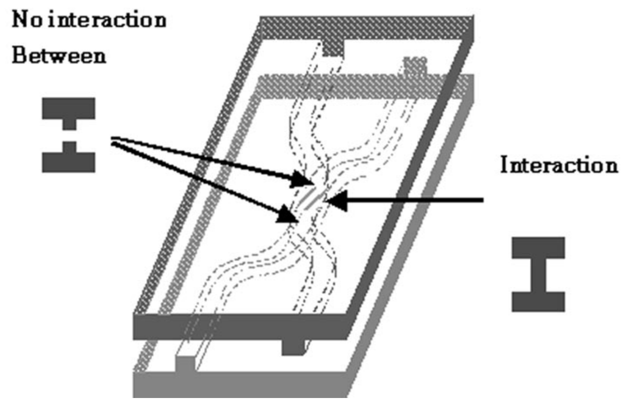

(a)

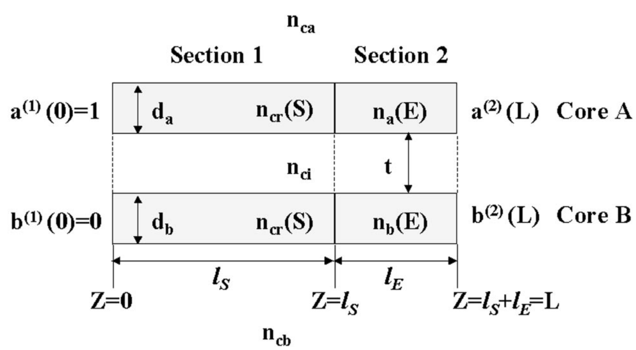

(b)

Fig. 1. (a) FVCSs with separated input and output waveguides. (b) Schematic diagram of one-dimensional (1–D) index profile in the straight interaction region of fused VDCSs with two sections.

Ultrashort vertical directional couplers have an inherent limitation in their extinction ratios due to nonorthogonality of individual waveguide modes [6]. One can improve extinction ratios for the cross state using slight asymmetry in the structure and that for the bar state using the combination of symmetric and asymmetric two-section structures [7], [8]. It was shown that both cross and bar states with high extinction ratios larger than 30 dB can be achieved at the same end of the ultrashort two-section fused vertical coupler switch (FVCS) by changing the refractive indexes of the inner-cladding layer and cores of less than 1% [9].

Manuscript received January 18, 2002; revised May 2, 2002. This work was supported in part by the Korean Ministry of Education through the BK21 project, by Advanced Photonics Technology, and by the Korea Science and Engineering Foundation (KOSEF) through the Ultra-Fast Fiber-Optic Networks Research Center at Kwangju Institute of Science and Technology.

S.-C. Cho and H. H. Hong are with the Optical Packet Routing Team, ETRI, Taejon 305-350, Korea.

B.-M. Jung and B.-G. Kim are with the School of Electronic Engineering, Soongsil University, Seoul 156-743, Korea.

A. Shakouri is with the Baskin School of Engineering, University of California, Santa Cruz, CA 95064 USA.

Digital Object Identifier 10.1109/JLT.2002.802215

For the structure of [9], in order to change the refractive indexes of the inner-cladding layer and cores independently by carrier injection or electrooptic effect, complex electrode structures and fabrication processes are necessary. In order to simplify the processing, one must reduce the number of layers in each section in which the refractive indexes need to be changed for switching operation and an improvement of extinction ratios. In this paper, we propose a vertical directional coupler switch (VDCS) with switching-operation-induced section and extinction-ratio-enhanced section with a length less than 400 μm. In these VDCSs, the switching operation was achieved by changing the refractive indexes of both cores in the switching-operation-induced section, and an improvement of extinction ratios larger than 30 dB for both cross and bar states was achieved by controlling the asymmetry of refractive indexes of two cores in the extinction-ratio-enhanced section without a need to change the refractive index of the inner-cladding layer. The required refractive indexes for the cores in the switching-operation-induced and extinction-ratio-enhanced sections are calculated for various thicknesses of the inner-cladding layer.

The transfer matrix method and the improved coupled-mode theory (ICMT) are used to analyze these structures, and the results are compared with those of the two–dimensional (2-D) finite-difference beam propagation method (BPM).

This paper is organized as follows. In Section II, the ICMT and the transfer matrix method are briefly described for multisection vertical directional couplers. In Section III, VDCSs with two sections are described. In Section IV, the design procedure and examples for VDCSs with two sections, which have both cross and bar states with high extinction ratios larger than 30 dB, are presented. The effect of the thickness of the inner-cladding layer on the refractive indexes of cores in two sections is investigated. Finally, conclusions are given in Section V.

II. ICMT and Transfer Matrix Method in Multisection Vertical Directional Couplers

The improved coupled-mode equations in the ith segment of a two-section vertical directional coupler, shown in Fig. 1, are given by [10]

$$\frac{d}{dz}a^{(i)}(z) = -i\gamma_{(a)}^{(i)}a^{(i)}(z) - ik_{ab}^{(i)}b^{(i)}(z) \tag{1}$$

and

$$\frac{d}{dz}b^{(i)}(z) = -ik_{ba}^{(i)}a^{(i)}(z) - i\gamma_{(b)}^{(i)}b^{(i)}(z) \tag{2}$$

where

$$\gamma_{(a)}^{(i)} = \beta_a^{(i)} + \frac{K_{aa}^{(i)} - C_{(i)}K_{ba}^{(i)}}{1 - C_{(i)}^2}$$

$$\gamma_{(b)}^{(i)} = \beta_b^{(i)} + \frac{K_{bb}^{(i)} - C_{(i)}K_{ab}^{(i)}}{1 - C_{(i)}^2}$$

$$k_{ab}^{(i)} = \frac{K_{ab}^{(i)} - C_{(i)}K_{bb}^{(i)}}{1 - C_{(i)}^2}$$

$$k_{ba}^{(i)} = \frac{K_{ba}^{(i)} - C_{(i)}K_{aa}^{(i)}}{1 - C_{(i)}^2}$$

$$K_{ab}^{(i)} = \frac{\omega}{4}\int\int \delta\varepsilon_{(q)}^{(i)}\left[\mathbf{E}_{t,a}^{(i)}\cdot\mathbf{E}_{t,b}^{(i)} - \mathbf{E}_{z,a}^{(i)}\cdot\mathbf{E}_{z,b}^{(i)}\right]dxdy$$

$$C_{(i)} = \frac{C_{ab}^{(i)} + C_{ba}^{(i)}}{2}$$

$$C_{ab}^{(i)} = \frac{1}{2}\int\int \mathbf{E}_{t,b}^{(i)}\times\mathbf{H}_{t,a}^{(i)}\cdot\hat{z}\,dxdy$$

$$C_{ba}^{(i)} = \frac{1}{2}\int\int \mathbf{E}_{t,a}^{(i)}\times\mathbf{H}_{t,b}^{(i)}\cdot\hat{z}\,dxdy.$$

$\mathbf{E}_{t,a}^{(i)}$ and $\mathbf{H}_{t,a}^{(i)}$ and $\mathbf{E}_{t,b}^{(i)}$ and $\mathbf{H}_{t,b}^{(i)}$ are the transverse electric (TE) and transverse magnetic (TM) fields of waveguides A and B in the ith section, respectively, and $a^{(i)}(z)$ and $b^{(i)}(z)$ are the mode amplitudes of waveguides A and B in the ith section, respectively.

The mode amplitudes at the end of section 2 of waveguides A and B, $a^{(2)}(L)$, and $b^{(2)}(L)$ can be expressed by the transfer matrix and are related to the mode amplitudes of waveguides A and B at the input of section 1, $a^{(1)}(0)$, and $b^{(1)}(0)$ as follows:

$$\begin{bmatrix} a^{(2)}(L) \\ b^{(2)}(L) \end{bmatrix} = T^{(2)}T^{(1)}\exp\left[-i\left(\phi^{(1)} + \phi^{(2)}\right)\right]\begin{bmatrix} a^{(1)}(0) \\ b^{(1)}(0) \end{bmatrix}. \tag{3}$$

where the transfer matrix in the ith section is given by

$$T^{(i)} = \begin{bmatrix} \cos\psi^{(i)}l^{(i)} + i\frac{\Delta^{(i)}}{\psi^{(i)}}\sin\psi^{(i)}l^{(i)} & -i\frac{k_{ab}^{(i)}}{\psi^{(i)}}\sin\psi^{(i)}l^{(i)} \\ -i\frac{k_{ba}^{(i)}}{\psi^{(i)}}\sin\psi^{(i)}l^{(i)} & \cos\psi^{(i)}l^{(i)} - i\frac{\Delta^{(i)}}{\psi^{(i)}}\sin\psi^{(i)}l^{(i)} \end{bmatrix} \tag{4}$$

where

$$\Delta^{(i)} = \frac{\gamma_b^{(i)} - \gamma_a^{(i)}}{2}$$

$$\psi^{(i)} = \sqrt{\Delta^{(i)2} + k_{ab}^{(i)}k_{ba}^{(i)}}$$

and $l^{(i)}$ is the length of each section.

The output powers at the end of each section for waveguides A and B, $P_a^{(i)}$, and $P_b^{(i)}$ are given by

$$P_a^{(i)} = \mathrm{Re}\left[\left(a^{(i)}\left(l^{(i)}\right) + C_{ab}^{(i)}b^{(i)}\left(l^{(i)}\right)\right) \times\left(a^{*(i)}\left(l^{(i)}\right) + C_{ab}^{*(i)}b^{*(i)}\left(l^{(i)}\right)\right)\right] \tag{5}$$

$$P_b^{(i)} = \mathrm{Re}\left[\left(C_{ba}^{(i)}a^{(i)}\left(l^{(i)}\right) + b^{(i)}\left(l^{(i)}\right)\right) \times\left(C_{ba}^{*(i)}a^{*(i)}\left(l^{(i)}\right) + b^{*(i)}\left(l^{(i)}\right)\right)\right]. \tag{6}$$

III. VDCSs With Switching-Operation-Induced and Extinction-Ratio-Enhanced Sections

From the analysis of two-section FVCs and FVCSs in [8] and [9], one can achieve the cross state with high extinction ratios larger than 30 dB using a one-section asymmetric coupler. In addition, one can achieve the bar state with high extinction ratios larger than 30 dB using two-section VDCSs with an asymmetric

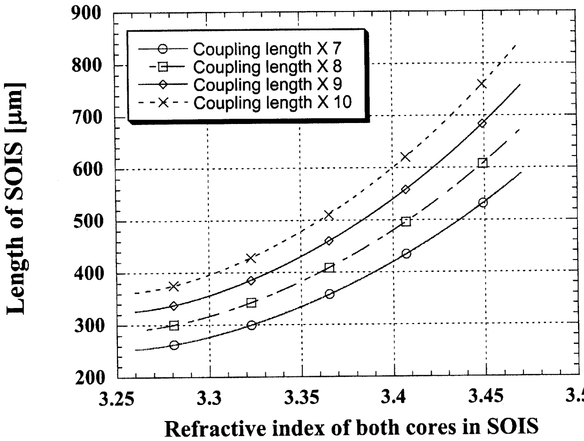

Fig. 2. Length of section 1 as a function of the refractive index of both cores for various multiples of coupling length in section 1 of vertical directional couplers with the thickness of the inner-cladding layer of 0.6 μm.

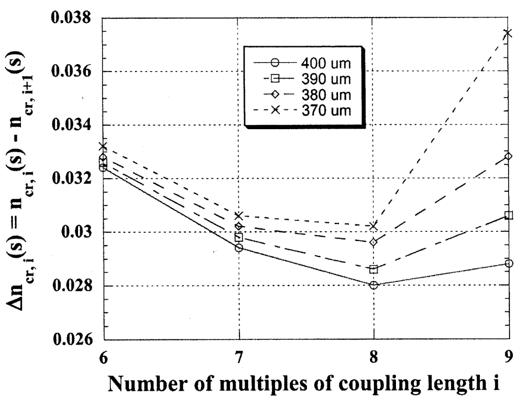

Fig. 3. Refractive index change of both cores for switching operation $\Delta n_{\mathrm{cr},i} = n_{\mathrm{cr},i} - n_{\mathrm{cr},i+l}$ for various lengths of section 1 with the thickness of the inner-cladding layer of 0.6 μm.

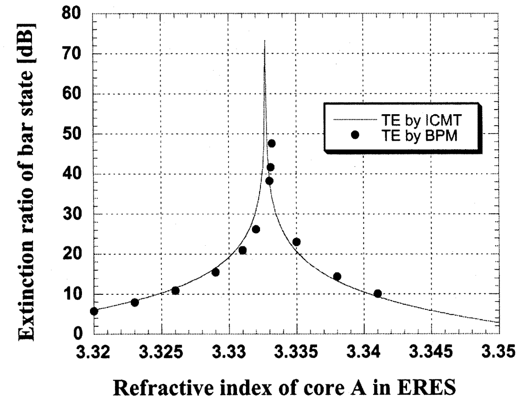

Fig. 4. Extinction ratio of bar state as a function of the refractive index of core A in section 2 with the refractive index of both cores in section 1 of 3.3118 and that of core B in section 2 of 3.3271. (The length of section 1 is 370 μm.)

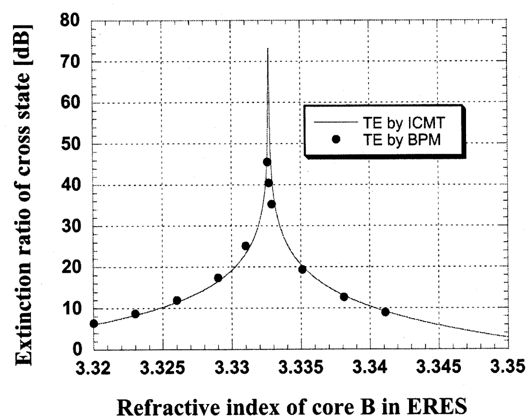

Fig. 5. Extinction ratio of cross state as a function of the refractive index of core B in section 2 with the refractive index of both cores in section 1 of 3.3424 and that of core A in section 2 of 3.3271. (The length of section 1 is 370 μm.)

coupler followed by a symmetric coupler, or vice versa. Extinction ratios for cross and bar states of symmetric couplers usually range from 13 to 18 dB at short coupling lengths in strongly coupled FVCs considered in this work [8]. With extinction ratios less than 18 dB at the end of section 1, one can achieve high extinction ratios larger than 30 dB at the end of section 2 using a slight asymmetry in refractive indexes of cores in section 2.

In order to reduce the number of layers whose refractive indexes should be changed for high-extinction-ratio switching operations for both cross and bar states, one can divide the VDCS into two functional sections. The first one (section 1) is the switching-operation-induced section, and it uses a symmetric coupler. The second one (section 2) is the extinction-ratio-enhanced section, and it uses an asymmetric coupler.

One notices that the refractive index of the core in which the power is launched is smaller than that of the other core to obtain high extinction ratios [8]. The extinction ratio of section 2 is mainly determined by the asymmetry of refractive indexes of two cores in section 2 and is not affected by refractive indexes of cores in section 1. Thus, to obtain the same asymmetry for high extinction ratios larger than 30 dB for both cross and bar states, one should choose the refractive index of both cores in section 2 as the average value of the refractive index of cores of cross and bar states in section 1. Then, the length of section 2 for the cross state is equal to that for the bar state.

In order to achieve switching operation and high extinction ratios for both cross and bar states, the control of the refractive index in both core regions of the waveguides is necessary. The required changes can be realized using electrooptic effect or carrier injection. With the appropriate doping profile and material composition or orientation, one can control the change in the refractive index of different regions independently. For example, Liu *et al.* have recently demonstrated a push–pull operation for a vertical coupler switch with the use of a single electrode [11].

In the VDCS with the switching-operation-induced and extinction-ratio-enhanced sections, one can achieve the switching operation and an improvement of extinction ratios without the change of the refractive index of the inner-cladding layer. Thus, the structure and fabrication process of the proposed VDCS with the switching-operation-induced and extinction-ratio-enhanced sections is simpler than that of an FVCS in [9].

IV. Simulation Results and Discussion

Fig. 1(a) shows the FVCS with separate input and output waveguides. The 2-D index profile of a vertical directional coupler is reduced to one dimension using the effective index

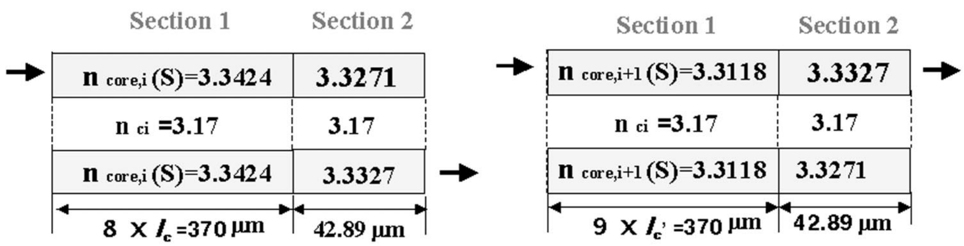

(a) (b)

Fig. 6. Design example of a two-section VDCS for output in (a) cross state and (b) bar state. The incident power is launched into core A.

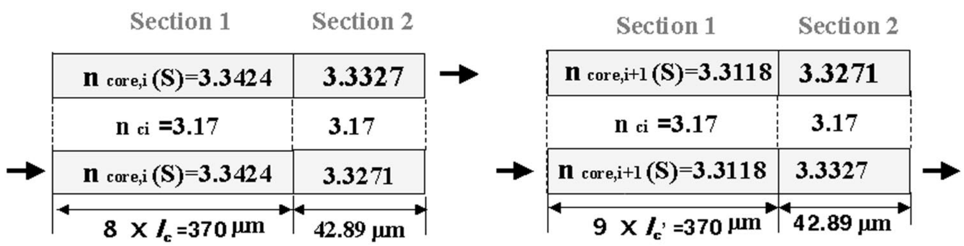

(a) (b)

Fig. 7. Design example of a two-section VDCS for output in (a) cross state and (b) bar state. The incident power is launched into core B.

method. The schematic diagram of a 1-D index profile of VDCSs with two sections is shown in Fig. 1(b). The results for TE mode are presented. The TM modes have a similar behavior. The parameter values used in the analysis are $n_{ca} = n_{cb} = n_{ci} = 3.17, d_a = d_b = 0.5$ μm, and $t = 0.6\,\mu$m, and the wavelength is $1.55\,\mu$m. We assume that the power is launched into core A in section 1. The extinction ratio of cross and bar states of the section i is defined as $P_b^{(i)}/P_a^{(i)}$ and $P_a^{(i)}/P_b^{(i)}$, respectively, where $P_a^{(i)}$ and $P_b^{(i)}$ are the guided mode powers at the end of each section of waveguides A and B, respectively.

The length of section 1 as a function of the refractive index of both cores for various multiples of coupling length is shown in Fig. 2. The thickness of the inner-cladding layer is taken to be 0.6 μm. In order to achieve both cross and bar states at the end of a VDCS, the length of section 1 should be chosen so that it is equal to $(m-1)l_c|_{n_{\rm cr}(S)|_{\rm MAX}} = ml_c'|_{n_{\rm cr}(S)|_{\rm MIN}}$. The coupling lengths l_c and l_c' are those of bar (cross) and cross (bar) states in section 1, respectively, if m is odd (even). The refractive index of both cores in section 1 is denoted by $n_{\rm cr}(S)$. Thus, the index difference, $\Delta n_{\rm cr} = n_{\rm cr}(S)|_{\rm MAX} - n_{\rm cr}(S)|_{\rm MIN}$ represents the change of the refractive index of both cores in section 1 necessary for the switching operation. One should design the VDCS in the region in which $\Delta n_{\rm cr}$ is less than 0.03 due to the assumption of the change of refractive index of cores less than 1%. Based on the above relationship, one can determine the refractive index of both cores in section 1 after choosing the length of section 1.

In order to determine the length and the refractive index of both cores of section 1, we calculate the difference of the refractive index between the multiples of coupling length for various lengths of section 1. Fig. 3 shows the refractive index change of both cores for switching operation $\Delta n_{{\rm cr},i} = n_{{\rm cr},i} - n_{{\rm cr},i+l}$ for various lengths of section 1 in VDCSs with the thickness of the inner-cladding layer of $0.6\,\mu$m, where $n_{{\rm cr},i}$ represents the

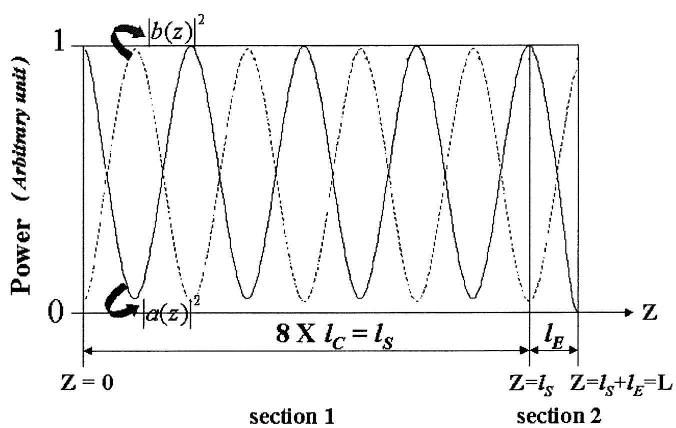

Fig. 8. Guided power inside waveguides A and B as a function of distance for the VDCS described in Fig. 6(a).

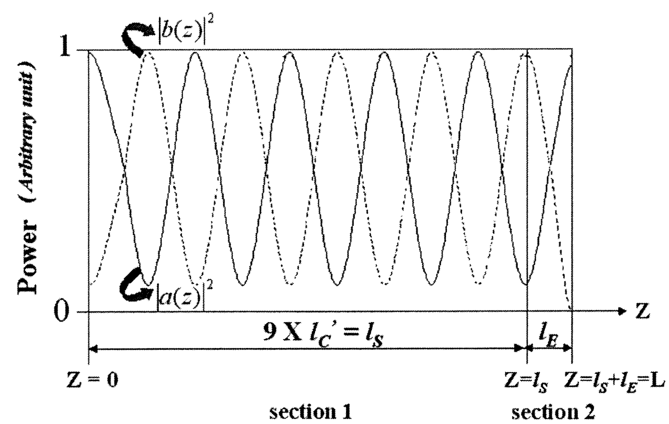

Fig. 9. Guided power inside waveguides A and B as a function of distance for the VDCS described in Fig. 6(b).

refractive index of both cores in section 1 when the multiple i of coupling length is equal to the length of 370, 380, 390, and

TABLE I
TOLERANCE OF THE REFRACTIVE INDEX AND THE OPTIMUM ASYMMMETRY OF CORES IN SECTION 2 AND THE REFRACTIVE INDEX CHANGE OF CORES IN SECTION 1 FOR SWITCHING OPERATION FOR VARIOUS THICKNESSES OF THE INNER-CLADDING LAYER

t [μm]	Length of section 1	$\Delta n_{cr}(S)$	Bar state (section 1)		Cross state (section 1)		(section 2)	
			m	$n_{cr}(S)$	m	$n_{cr}(S)$	$\delta n_{cr}\|_{>30\,dB}$	$\Delta n_{asy}(E)$
0.4	390 μm	0.0282	13	3.4232	14	3.3950	0.0021	0.0065
		0.0286	13	3.4232	12	3.4518	0.0019	0.0049
		0.0299	11	3.4817	12	3.4518	0.0017	0.0046
0.5	390 μm	0.0292	11	3.3566	12	3.3274	0.0019	0.0076
		0.0284	11	3.3566	10	3.385	0.0016	0.0048
		0.029	9	3.4140	10	3.385	0.0014	0.0037
0.6	390 μm	0.0306	9	3.3262	10	3.2956	0.0017	0.0073
		0.0286	9	3.3262	8	3.3548	0.0014	0.0046
		0.0298	7	3.3846	8	3.3548	0.0012	0.0029

400 μm, respectively. Based on the results shown in Fig. 3, one can determine the refractive index of both cores in section 1 after choosing the length of section 1. For example, one considers the case in which the length of section 1 is chosen to be 370 μm. In this case, the coupling lengths for cross and bar states satisfy that $8l_c = 9l'_c = 370\,\mu$m, and the refractive indexes of both cores for cross and bar states are 3.3424 and 3.3118, respectively. The refractive index change in section 1 for the switching operation in this case is 0.03 less than 1% of the refractive indexes of cores.

Extinction ratios of section 2 are mainly determined by the asymmetry of refractive indexes of two cores in section 2. To obtain the same coupling length and the same asymmetry for high extinction ratios larger than 30 dB for both cross and bar states in section 2, we choose the refractive index of both cores in section 2 as the average value of the refractive index of cores of cross state and bar state in section 1. In the case of the length of section 1 of 370 μm, we choose the refractive index of both cores in section 2 as $(3.3424 + 3.3118)/2 = 3.3271$.

Fig. 4 shows the extinction ratio of bar state as a function of the refractive index of core A in section 2 with the refractive index of both cores in section 1 of 3.3118 and that of core B in section 2 of 3.3271. The length of section 2 is 42.89 μm for the refractive index of core A of 3.3327 at which the maximum extinction ratio occurs. In this case, since the power is launched into core B in section 2, the refractive index of core A in section 2 is larger than that of core B in section 2 to obtain high extinction ratios larger than 30 dB. The refractive index difference between core B and core A for the maximum extinction ratio is 0.0056. The tolerance of the refractive index of core A in section 2, which gives the extinction ratios larger than 30 dB, is 0.0016.

Fig. 5 shows the extinction ratio of cross state as a function of the refractive index of core B in section 2 with the refractive index of both cores in section 1 of 3.3424 and of core A in section 2 of 3.3271. Since the asymmetry of the refractive index of both cores in section 2 for the maximum extinction ratio is the same as that in the case of Fig. 4, the length of section 2 for the refractive index of core B of 3.3327 at which the maximum extinction ratio occurs is equal to that of Fig. 4. Thus, the device length of the cross state is exactly equal to that of the bar state. Similar to the case of Fig. 4, the tolerance of the refractive index of core B in section 2 is 0.0016.

Fig. 6 shows an example of a VDCS with two sections designed based on the results in Figs. 3 –5 when incident power is launched into core A. Fig. 7 shows an example of a VDCS with two sections when incident power is launched into core B. The length of section 1 is 370 μm, and that of section 2 is 42.89 μm. Comparing the two figures, we can see that the refractive indexes of both cores in section 1 are the same, while the refractive index of core A in section 2 in Fig. 6 is equal to the index of core B in section 2 in Fig. 7, and vice versa.

Figs. 8 and 9 show the guided powers inside waveguide A and waveguide B as a function of distance for a VDCS based on the design in Figs. 6(a) and (b), respectively. We can clearly see that the extinction ratio is enhanced in section 2 due to the asymmetry of refractive indexes of the two cores in this section.

In order to investigate the effect of the thickness of the inner-cladding layer on the refractive indexes of cores in sections 1 and 2, the tolerance of the refractive index and the optimum asymmetry of cores in section 2, as well as the refractive index change of cores in section 1 required for switching operation in the case of the length of section 1 of 390 μm for various thicknesses of the inner-cladding layer, are calculated and summarized in Table I. The refractive index and the change of the refractive index of both cores required for switching operation in section 1 are denoted by $n_{\rm cr}(S)$ and $\Delta n_{\rm cr}(S)$, respectively. The optimum asymmetry (the refractive index difference between both cores at which the maximum extinction ratio occurs) in section 2 and the tolerance of the refractive index of cores in section 2 are denoted by $\Delta n_{\rm asy}(E) = |n_a(E) - n_b(E)|$ and $\delta n_{\rm cr}|_{>30\ \rm dB}$, respectively. The number of multiples of coupling length is denoted by m.

As can be seen in Table I, the refractive indexes of both cores in section 1 for cross and bar states increase and the refractive index change for switching operation decreases for the same length of section 1 as the inner-cladding layer thickness decreases. The tolerance of refractive indexes of cores in section 2 increases as the inner-cladding layer thickness decreases. The optimum asymmetry of section 2 is much less than 1% of the refractive index of cores, regardless of the thickness of the inner-cladding layer.

V. Conclusion

VDCSs with switching-operation-induced and extinction-ratio-enhanced sections with a length less than 400 μm have been proposed. In these VDCSs, switching operation was achieved by changing the refractive indexes of both cores in the switching-operation-induced section, and an improvement of extinction ratios larger than 30 dB for both cross and bar states was achieved by controlling the asymmetry of refractive indexes of two cores in the extinction-ratio-enhanced section without changing the refractive index of the inner-cladding layer. The effect of the thickness of the inner-cladding layer on the refractive indexes of cores in the switching-operation-induced and extinction-ratio-enhanced sections has been investigated.

References

[1] D. Sadot and I. Elhanany, "Optical switching speed requirements for terabit/second packet over WDM networks," *IEEE Photon. Technol. Lett.*, vol. 12, pp. 440–442, Apr. 2000.

[2] H. Inoue, T. Kato, Y. Takahashi, E. Amada, and K. Ishida, "InP-based optical switch module operating through carrier-induced refractive index change," *Opt. Eng.*, vol. 29, no. 3, pp. 191–199, 1990.

[3] R. F. Kalman, L. G. Kazovsky, and J. W. Goodman, "Space division switches based on semiconductor optical amplifiers," *IEEE Photon. Technol. Lett.*, vol. 4, pp. 1048–1051, Sept. 1992.

[4] A. Shakouri, B. Liu, B.-G. Kim, P. Abraham, A. W. Jackson, A. C. Gossard, and J. E. Bowers, "Wafer-fused optoelectronics for switching," *J. Lightwave Technol.*, vol. 16, pp. 2236–2242, Dec. 1998.

[5] M. M.-K. Liu, *Principles and Applications of Optical Communications*. Chicago, IL: IRWIN, 1996, ch. 11.

[6] K. L. Chen and S. Wang, "Cross-talk problems in optical directional couplers," *Appl. Phys. Lett.*, vol. 44, pp. 166–168, 1984.

[7] B.-G. Kim, A. Shakouri, B. Liu, and J. E. Bowers, "Improved extinction ratio in ultra short directional couplers using asymmetric structures," *Jpn. J. Appl. Phys.*, vol. 37, no. 8A, pp. L930–L932, 1998.

[8] S.-C. Cho, B.-G. Kim, and A. Shakouri, "High extinction ratios for cross and bar states in ultra short vertical directional couplers composed of two sections," *Jpn. J. Appl. Phys. 1 Regul. Rap. Short Notes*, vol. 39, no. 12A, pp. 6555–6559, 2000.

[9] S.-C. Cho, B.-G. Kim, Y. Moon, and A. Shakouri, "Ultra short two-section vertical directional coupler switches with high extinction ratios," *Jpn. J. Appl. Phys. 1 Regul. Rap. Short Notes*, vol. 40, no. 6A, pp. 4054–4050, 2001.

[10] S. L. Chuang, *Physics of Optoelectronic Devices*. New York: Wiley, 1995, pp. 302–305.

[11] B. Liu, A. Shakouri, P. Abraham, and J. E. Bowers, "Push–pull vertidal directional coupler switch," *IEEE Photon. Technol. Lett.*, vol. 11, pp. 662–664, June 1999.

[12] Q.-Y. Tong and U. Gosele, *Semiconductor Wafer Bonding (Science and Technology)*. New York: Wiley-Interscience, 1999.

Sung-Chan Cho, photograph and biography not available at the time of publication.

Byung-Min Jung, photograph and biography not available at the time of publication.

Boo-Gyoun Kim (M'90), photograph and biography not available at the time of publication.

Hyun Ha Hong, photograph and biography not available at the time of publication.

Ali Shakouri (M'01), photograph and biography not available at the time of publication.